ELSEVIER

Journal of Fluids and Structures 25 (2009) 80–94

JOURNAL OF FLUIDS AND STRUCTURES

www.elsevier.com/locate/jfs

Flow-excited acoustic resonance of two side-by-side cylinders in cross-flow

R. Hanson, A. Mohany, S. Ziada*

Department of Mechanical Engineering, McMaster University, 1280 Main Street West, Hamilton, Ontario, Canada L8S 4L7

Received 14 December 2006; accepted 20 March 2008
Available online 21 May 2008

Abstract

The aeroacoustic response of two side-by-side circular cylinders in cross-flow is investigated experimentally. In order to investigate the effect of the gap between the cylinders on the acoustic resonance mechanism, six spacing ratios between the cylinders, in the range of $T/D = 1.25$–3, have been investigated, where D is the diameter of the cylinders and T the centre-to-centre distance between them. Special attention is given to the intermediate spacing ratio range, which exhibits bistable flow regimes in the absence of resonance. During the tests, the acoustic cross-modes of the duct housing the cylinders are self-excited. For the intermediate spacing ratios, $T/D = 1.25$, 1.35, 1.46 and 1.75, two distinct vortex-shedding frequencies at the off-resonance conditions are observed. These are associated with the wide and narrow wakes of the cylinders, as described in the literature. In this case, acoustic resonances occur at a Strouhal number, which is between those observed before the onset of resonance. The acoustic resonance synchronizes vortex shedding in the two wakes and thereby eliminates the bistable flow phenomenon. For large spacing ratios, $T/D = 2.5$ and 3, vortex shedding occurs at a single Strouhal number at which the acoustic resonance is excited.

Keywords: Side-by-side cylinders; Vortex shedding; Acoustic resonance; Flow–acoustic interaction

1. Introduction

The phenomenon of flow-excited acoustic resonance is a design concern in many engineering applications, especially when separated shear flows are encountered in ducts, piping systems or other confined volumes. Typical examples of industrial equipments, which often experience flow-excited acoustic resonance, include tube bundles of heat exchangers and boiler plants (Fitzpatrick, 1986; Blevins and Bressler, 1993; Oengoeren and Ziada, 1998; Ziada, 2006), cascades of compressor blades (Parker and Pryce, 1974; Stoneman et al., 1988; Ziada et al., 2002), control valves (Ziada et al., 1989), and piping systems (Hourigan et al., 1990; Bruggeman et al., 1991; Ziada et al., 2006). The sound pressure generated by the resonant acoustic modes can be sufficiently high to cause structural failures, such as that reported recently for the steam dryer of BWR (NRC, 2003). Even when structural failure is not a concern, the sound pressure level (SPL) generated by the resonant mode often exceeds the allowable noise level in the work place and neighbouring communities.

*Corresponding author. Tel.: +1 905 525 9140; fax: +1 905 572 7944.
E-mail address: ziadas@mcmaster.ca (S. Ziada).

0889-9746/$ - see front matter © 2008 Elsevier Ltd. All rights reserved.
doi:10.1016/j.jfluidstructs.2008.03.008

Nomenclature

c	speed of sound
D	cylinder diameter
f_a	frequency of the lowest acoustic resonance mode of the test section
f_v	vortex-shedding frequency
h	height of the duct
L	centre-to-centre distance between two tandem cylinders
M	Mach number
n	acoustic mode number
P_{rms}	sound pressure (root mean square amplitude)
P^*	normalized sound pressure
SPL	sound pressure level
St	Strouhal number of vortex shedding
T	center-to-center distance between two side-by-side cylinders
U	upstream flow velocity
U_R	reduced velocity
u	particle velocity of the acoustic resonant mode
X	downstream distance from the cylinder axis
Y	vertical distance from the centre point between the two cylinders

Greek letters

λ	wavelength of the acoustic wave
ρ	air density

Tube bundles exposed to gas cross-flow in large containers are particularly liable to the mechanism of acoustic resonance. Although this phenomenon has received considerable attention in the literature, the effects of tube spacing and pattern on the excitation mechanism are still not well understood, *especially for tightly packed tube bundles*. For the case of a single cylinder in cross-flow, the acoustic resonance mechanism is relatively well understood; see for example Blevins (1985), Blevins and Bressler (1993) and Mohany and Ziada (2007). However, for the more complex case of *multiple cylinders in close proximity*, this resonance mechanism has received very little attention. Even for the relatively "simple" geometry of two cylinders in close proximity, the acoustic resonance mechanism has not been investigated until recently.

For a single cylinder in cross-flow, Blevins (1985) showed that applying *external* sound in a direction perpendicular to the mean flow had the effect of organizing the wake flow, increasing the spanwise correlation and essentially synchronizing and strengthening the vortex-shedding process. Hall et al. (2003) studied the effect of external sound on vortex shedding from two tandem cylinders and showed that the lock-in region is much wider than in the case of a single cylinder, which indicates that tandem cylinders in close proximity are much more liable to the acoustic resonance mechanism. For the *self-excited* case, Blevins and Bressler (1993) found the acoustic resonance of a single cylinder to occur in a classical manner, in which the resonance is initiated when the frequency of vortex-shedding approaches the acoustic mode frequency. This may generate a lock-in range of flow velocity over which the acoustic resonance is excited. Therefore, the lock-in for this case always occurs near the condition of frequency coincidence. In the tandem cylinders case, a similar acoustic resonance was observed by Mohany and Ziada (2005) at flow velocities near the condition of frequency coincidence. They designated this resonance range as the *coincidence range*. They also observed a new resonance phenomenon that occurred at flow velocities much lower than that corresponding to the frequency coincidence. This resonance, which they designated as the *pre-coincidence resonance*, is found to be controlled by the instability of the flow in the gap between the cylinders. Mohany and Ziada (2006) found the pre-coincidence resonance to be persistent for spacing ratios in the range between $L/D = 1.25$ and 3, where L is the centre-to-centre distance between the cylinders and D the diameter. It is therefore clear that the addition of a cylinder in the wake of another generates a new resonance phenomenon that could neither be predicted from single cylinder data nor from the non-resonant data of two tandem cylinders. The objective of the present study is to investigate the *effect of proximity on the acoustic resonance mechanism of two side-by-side cylinders.*

Cross-flow over two side-by-side circular cylinders has been a topic of ongoing research for many years because of its relevance to many engineering applications. It is generally accepted that the behaviour of the flow in this case is strongly dependent on the distance between the cylinders and, to a lesser extent, on the Reynolds number. The spacing between the cylinders is conventionally expressed by the spacing ratio T/D, where T is the distance between the centres of the cylinders and D the diameter.

Several authors observed bistable flow regimes in the wake of two side-by-side cylinders with spacing ratios in the range of $T/D = 1.2$–2.2, see for example, Bearman and Wadcock (1973) and Kim and Durbin (1988). These regimes are generated by flow bias, or asymmetry, which produces a wide near-wake region behind one cylinder and a narrow near-wake region behind the other, as illustrated in Fig. 1(a). The narrow and wide wakes switch back and forth between the two cylinders and produce two vortex-shedding frequencies. On the other hand, cylinders with larger spacing ratios,

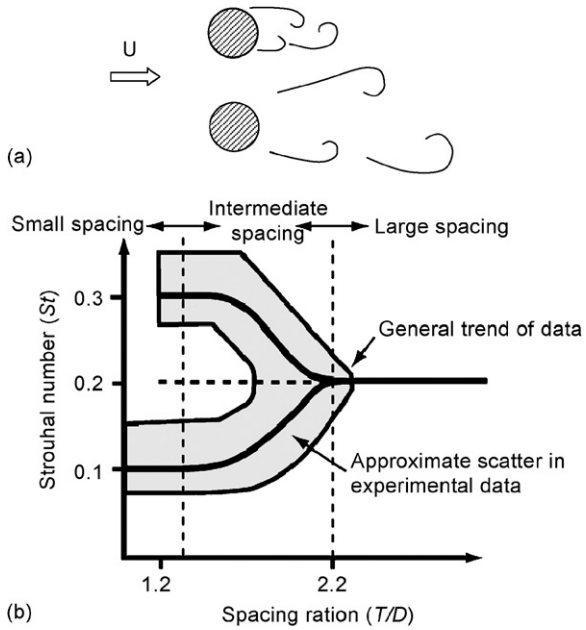

Fig. 1. (a) Schematic illustration of the bistable biased wake flow behind two side-by-side cylinders in cross-flow. (b) Schematic illustration of the effect of the spacing ratio on the Strouhal number of vortex shedding from two side-by-side cylinders in cross-flow.

$T/D > 2.2$, do not exhibit these bistable flow properties. Instead, the wakes appear more symmetric and become dominated by vortex shedding at a single frequency. The spacing ratio separating the bistable and stable flow regimes depends on the Reynolds number.

Sumner et al. (1999) investigated side-by-side cylinders exposed to cross-flow and presented their results together with those reported by other researchers, such as Bearman and Wadcock (1973) and Kim and Durbin (1988). The general trend of the Strouhal number data and the degree of data scatter are illustrated schematically in Fig. 1(b). In this figure, the Strouhal number is defined by

$$\mathrm{St} = \frac{f_v D}{U}, \tag{1}$$

where f_v is the vortex-shedding frequency and U the approach flow velocity. For spacing ratios in the range $T/D = 1.2$–2.2, there are two distinct vortex-shedding frequencies corresponding to the bistable flow regimes. The high vortex-shedding frequency is associated with the narrow-closed wake and the low shedding frequency is generated by the wide-open wake. As can be seen in Fig. 1(b), there is a considerable scatter in the data due to different test conditions, but the general trend is consistent in all experiments.

Kim and Durbin (1988) investigated the effect of sound on the bistable flow of two side-by-side cylinders in cross-flow. They used a loud speaker, positioned at the wind tunnel entrance, to excite the flow at the instability frequency of the shear layers separating from the cylinders. This frequency is typically 6–8 times higher than the vortex-shedding frequencies in the cylinder wake, which correspond to the Strouhal number chart given in Fig. 1. This type of excitation was found to eliminate the bistable flow regime. Symmetric steady mean flow existed during excitation of cases that normally would have been asymmetric. Alam et al. (2003) employed wavelet analysis to explore the bistable nature of the wake of two side-by-side cylinders. They reported that the switching phenomenon of the bistable wake produces an intermediate Strouhal number. However, it is not clear why this switching process generates a single intermediate value of the Strouhal number instead of producing a range of Strouhal numbers extending between the high and low values observed during the bistable flow in the wake.

This brief summary of previous work, together with Fig. 1, highlights the complexity of the flow in the wake of two side-by-side cylinders in cross-flow. It is clear that as the spacing ratio T/D is altered, different flow regimes and vortex-shedding mechanisms are generated in the wake. The objective of this paper is to investigate the ability of this biased and bistable wake pattern to excite acoustic resonances of the duct housing the cylinders. To that end, special attention is devoted to the acoustic resonance mechanism for the range of spacing ratios corresponding to the bistable flow regimes in the wake, i.e. for $T/D = 1.2$–2.2.

2. Experimental set-up

A schematic of the test-section housing the two side-by-side cylinders is shown in Fig. 2. This arrangement was connected to the suction side of a 50 HP centrifugal blower. A variable speed controller was used to vary the flow velocity in the test-section up to 110 m/s. At the test-section inlet, a parabolic contraction was used. Preliminary experiments showed that the flow in the test-section was uniform within 2%. A diffuser and a flexible duct were used to connect the test-section outlet to the blower suction side. This arrangement reduced vibration transmission from the blower to the test section. The test-section was 812 mm long and its cross-section was 254 mm in height and 76 mm in width. In order to investigate the effect of the spacing between the cylinders, T, on the acoustic resonance mechanism, six spacing ratios between the cylinders were tested. These spacing ratios were in the range of $T/D = 1.25$–3. The cylinders had a diameter of $D = 21.8$ mm, and were machined from aluminium to produce a smooth finish. This arrangement yielded a total blockage ratio of 17%, due to the presence of the two cylinders, and an aspect ration of 3.5 for the cylinders. The relatively large flow blockage and short cylinder length were necessary to ensure coincidence of the vortex-shedding frequency with the acoustic mode frequency at sufficiently high flow velocities. As discussed by several authors, for example by Fitzpatrick (1986), Blevins and Bressler (1993) and Mohany and Ziada (2006), frequency coincidence at a sufficiently high flow velocity is a necessary condition for the generation of self-excited acoustic resonances. This necessity was confirmed by means of preliminary tests with smaller diameter cylinders, to reduce the flow blockage and increase the aspect ratio. In these preliminary tests, self-excited acoustic resonances could not be generated within the tested range of flow velocity. It should be noted here that the measured Strouhal numbers were generally within the range of published data in the literature, Fig. 1, albeit somewhat higher than the mean value because of the large blockage ratio. It is noteworthy also that the correlation length of vortex shedding at flow conditions near acoustic resonances is of the order of one cylinder diameter (Norberg, 2003). However, and more importantly for the present investigation, the main flow characteristics, including the *bistable biased* flow features, were found to be similar to those observed in previous studies. Based on these preliminary results, it was concluded that this test set-up is adequate for the present study because the main objective is to investigate *the interaction mechanism of the bistable biased flow with the acoustic mode*, rather than to measure the Strouhal number of vortex shedding which is already well documented in the literature. As will be shown later, both the bistable and biased flow phenomena have been exhibited, beyond doubt, by the present test set-up.

Dismountable windows were provided on the sidewalls of the test-section to set various spacing ratios between the cylinders and to ensure accurate alignment of the cylinders. This alignment is crucial for observing the bistable flow as noted by Price and Paidoussis (1984). The cylinders had a hole tapped in each end to provide a means to rigidly hold them in place.

The frequency of the acoustic cross-modes, see Fig. 2, can be approximated by

$$f_a = \frac{nc}{2h}, \tag{2}$$

where f_a is the acoustic mode frequency, n the mode number (1, 2, 3,…), c the speed of sound in the flowing medium and h the height of the test-section. For the first mode, $n = 1$, this corresponds to a frequency of approximately 688 Hz. This acoustic mode was excited in the present tests at flow velocities near 70 m/s, which corresponds to a Reynolds number of 10^5.

To measure the SPL, a 1/4″ condenser microphone was used along with a preamplifier and a power supply, all of which are type G.R.A.S. The microphone was mounted flush against the top acrylic plate of the test-section. The optimal location of the microphone was based on the work of Mohany and Ziada (2005). The microphone was calibrated using a G.R.A.S sound calibrator type 42AB. A Dantec 55P11 hot-wire probe in conjunction with Dantec Type 55M01 CTA were used to measure the fluctuating velocity in the wake of the cylinders. A PCI-4452 four channel, 16-bit data acquisition system was used to digitize the signals from the microphone and hot-wire probe. The data was sampled at 16,384 Hz for 60 s. The spectrum was obtained by averaging 1 s blocks for both the hot-wire and microphone measurements. Mean velocity of upstream flow as well as hot-wire calibrations were conducted with the aid of a pitot static tube.

The hot-wire probe was positioned at an X/D value between 1.5 and 2 diameters downstream of the cylinders and outside the interference zone between the two cylinders as shown in Fig. 3. The selection of this position was based on the finding of previous researchers. For example, it is known that the formation length of the vortices decreases with increasing the Reynolds number and therefore the frequency from the narrow wake structure may not be detected at greater downstream distances (Xu et al., 2003). Kim and Durbin (1988) also measured the vortex-shedding frequency at a similar position, i.e. outside the interference zone, to minimize the effect of the probe in disturbing the flow. The probe transverse position Y/D was varied with each spacing ratio because the wake pattern changed with the spacing ratio.

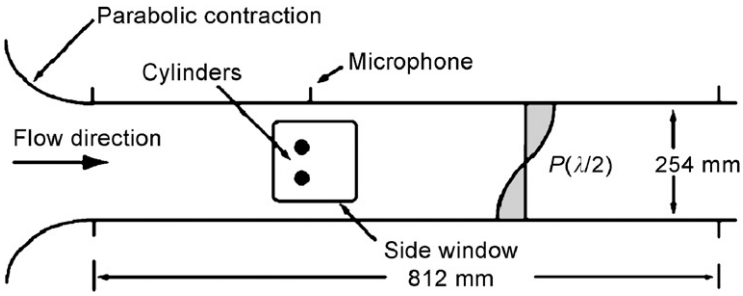

Fig. 2. Schematic of the test section showing the acoustic pressure distribution of the first cross-mode of the duct, $P(\lambda/2)$.

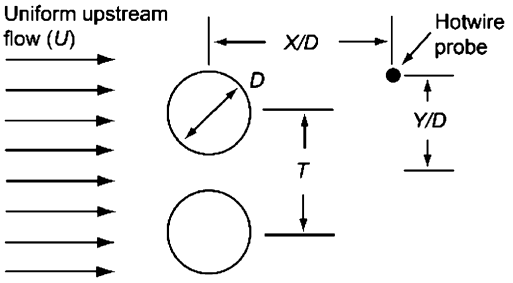

Fig. 3. Definition of the spacing ratio, T/D, and the placement of the hot-wire probe.

These variations were necessary to ensure capturing of all frequency components in the wake of the cylinders. For each spacing ratio, the hot-wire was used to document the Strouhal number(s) of vortex shedding. However, when the acoustic response was being investigated, the hot-wire probe and its holder were removed from the test section because it was observed that the acoustic resonance was somewhat weaker in the presence of the hot-wire. Once the acoustic response of the system was characterized, simultaneous hot-wire and microphone measurements were performed to investigate the flow behaviour as the acoustic resonance mechanism is developed with increasing flow velocity.

In order to capture the bistable flow phenomenon, which persists before the onset of resonance, the hot-wire probe was placed at $X/D = 1.5$ downstream of the cylinders and at $Y/D = 0.55$. This location is at the upper edge of the jet issuing from the gap between the cylinders, and therefore the hot-wire signal from this location can be used to distinguish both bistable flow patterns. For one flow pattern, it would be located in the jet formed between the cylinders, but when the flow switches to the other pattern, it would be positioned inside the wide wake of one cylinder. As will be seen latter, this procedure was adequate to capture the flip-flop nature of the wake flow. Kim and Durbin (1988) used a different technique to observe this phenomenon. They measured the change in the angle of the jet, by means of a cross-wire probe, and recorded the change in the cylinder base pressures.

The experiments were performed as follows. First, spectra of the sound pressure were measured, without the hot-wire probe in place, over the total range of flow velocities, extending from 6 to 110 m/s. This velocity range corresponds to a Reynolds number range between 9×10^3 and 1.6×10^5; thus extending into the high sub-critical regime. Following these measurements, the hot-wire was installed and the experiments were repeated to accurately determine the vortex-shedding frequencies from the hot-wire signal as a function of flow velocity. This procedure was necessary because the pressure spectra taken by the microphone on the top wall of the test section did not always display well-defined peaks at the vortex-shedding frequency.

3. Investigated geometries and dimensionless parameters

Based on the Strouhal number chart shown in Fig. 1, several spacing ratios corresponding to different flow regimes have been investigated. These include two cases with large spacing ratios, $T/D = 2.5$ and 3. Since the results of both cases are found to be similar, only the case with $T/D = 2.5$ will be addressed here for the sake of brevity. This spacing ratio will be addressed first because its aeroacoustic behaviour has been found to exemplify the classical mechanism of

vortex-induced acoustic resonance, which is similar to that observed for the case of an isolated cylinder (Blevins and Bressler, 1993; Mohany and Ziada, 2005).

The smallest spacing ratio that has been examined, $T/D = 1.25$, is very close to the boundary between the small and the intermediate spacing regimes, as can be seen from Fig. 1(b). This geometry will be considered in the second place because its aeroacoustic response is found to be rather different from that observed for the large spacing case with $T/D = 2.5$. The other tested cases with $T/D = 1.46$ and 1.75 are inside the intermediate spacing range. The results of these cases will be presented last to show the transition of the acoustic resonance mechanism as the spacing between the cylinders is increased from the small to the large spacing range.

For each case, see Fig. 4 as an example, the aeroacoustic response is presented by means of plots of the vortex-shedding frequency, f_v, versus the reduced velocity which is defined as

$$U_R = \frac{U}{f_a D}, \tag{3}$$

where U is the free-stream velocity and f_a the frequency of the first acoustic mode. Note that the slope of this plot is proportional to the Strouhal number, St.

Directly below the vortex-shedding frequency plot, the normalized acoustic pressure of the first acoustic mode is given as a function of the reduced velocity. Based on the theory of aerodynamic sound (Lighthill, 1952), the sound generated by an eddy in a coherent flow structure is proportional to the eddy length scale, the dynamic head and Mach number. Therefore, the dynamic head and Mach number, M, are used to normalize the acoustic pressure as follows:

$$P^* = \frac{P_{\text{rms}}}{\frac{1}{2}(\rho U^2 M)}, \tag{4}$$

where P_{rms} is the root-mean-square amplitude of the acoustic pressure and ρ the density of air. As reported by Mohany and Ziada (2005), Eqs. (3) and (4) were found to normalize the acoustic resonance response curve of isolated cylinders, with different diameters, exposed to cross-flow.

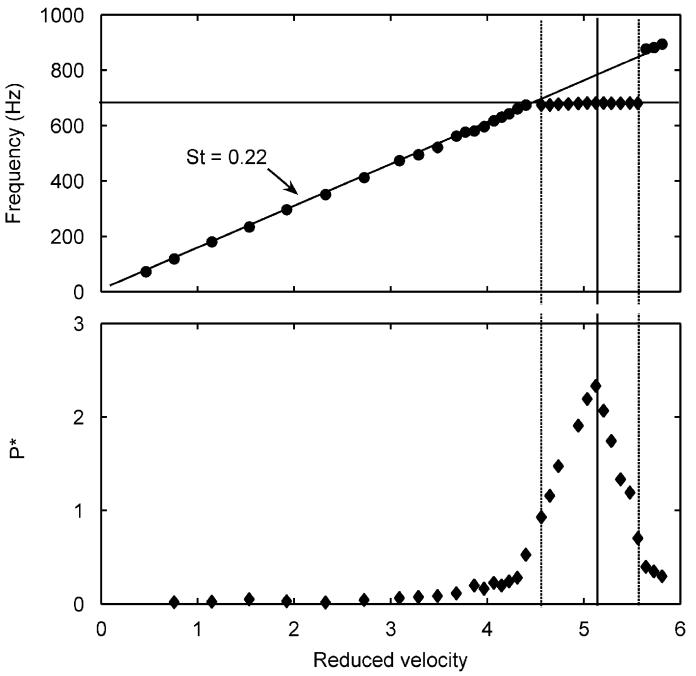

Fig. 4. The aeroacoustic response of the two side-by-side cylinders with $T/D = 2.5$ and $D = 21.8$ mm: ●, vortex-shedding frequency; ◆, first resonance mode frequency and magnitude.

4. Results of the large spacing cases

For the larger spacing ratios, $T/D = 2.5$ and 3.0, only one vortex-shedding component was present at any velocity of the tested velocity range, up to 90 m/s. In this case, the flow is *not* expected to be biased, since there is only one shedding frequency, and the widths of both wakes are expected to be approximately equal. This is consistent with the results in the literature for similar spacing ratios, as summarized by Sumner et al. (1999). Typical results showing the aeroacoustic response for the case with $T/D = 2.5$ are shown in Fig. 4. As mentioned earlier, the results of the case with $T/D = 3$ are not discussed here because they are similar to those shown in Fig. 4. The Strouhal number for each of the larger spacing ratios was 0.22, which is within the data range given in the literature.

As shown in Fig. 4, the vortex-shedding frequency increases linearly with the flow velocity, which is similar to the case of vortex shedding from an isolated cylinder. No "frequency jump" occurs when the first acoustic mode is initiated and the sound pressure increases gradually within the lock-in resonance range. Approximately at the centre of the lock-in region, the acoustic pressure reaches a maximum value of $P^* = 2.33$; corresponding to an acoustic pressure of 1860 Pa or 159 dB. As the flow velocity is increased further, the acoustic resonance subsides and the vortex-shedding frequency reverts back to the natural Strouhal number of 0.22.

In Fig. 5, several sample spectra of hot-wire and microphone signals are presented. These spectra were measured simultaneously at several flow velocities corresponding to: the pre-resonance range (Figs. 5(a) and (b)); the maximum acoustic pressure (Fig. 5(c)); and the post-resonance range (Fig. 5(d)). The reduced velocity given for each pair of spectra corresponds to the results shown Fig. 4. From the microphone data, the peak at the first mode resonance frequency is clearly visible in each spectrum at approximately 680 Hz. Additional low-frequency peaks can be seen at low flow velocities in the microphone spectra only, e.g. Fig. 5(a). These pressure peaks, which have low frequencies and small amplitudes, correspond to longitudinal modes of the tunnel and do not interfere with acoustic resonance mechanism of the transverse mode of the test section, which is being investigated here.

At the pre-resonance conditions, the microphone spectrum shows that the first acoustic mode of the duct is very weakly excited by the broadband turbulence in the wake of the cylinders. The response amplitude of the acoustic mode increases as the vortex-shedding frequency approaches that of the first more. At resonance conditions, the first acoustic mode dominates both the hot-wire and microphone spectra. In the post lock-in range (Fig. 5(d)), the vortex-shedding frequency component is seen to be recovered and corresponds to the Strouhal number observed before the onset of acoustic resonance.

As mentioned earlier, these observations are typical of classical vortex-induced acoustic resonance mechanism, including the lock-in phenomenon during which the acoustic particle velocity of the resonant mode locks-in the vortex-shedding frequency over a certain range of flow velocity. The wake structure during acoustic resonance in this case is expected to be synchronized by the resonant acoustic particle velocity (u) as shown schematically in Fig. 6; see, for example, Oengoeren and Ziada (1992).

5. Results of the small spacing case

The flow characteristics for the smallest spacing ratio, $T/D = 1.25$, differ from those exhibited by the large spacing cases as described above. In this case, two vortex-shedding frequencies are distinguished in the pre-resonance range. These frequencies are generated by the narrow and wide wakes, as discussed in the Introduction.

As the flow velocity is increased, a wide lock-in region occurs due to the resonance of the first acoustic mode. This wide lock-in is illustrated in Fig. 7, which shows a waterfall plot of the acoustic pressure spectra as the flow velocity is varied. The maximum acoustic pressure occurs at a flow velocity near 75 m/s, corresponding to a reduced velocity of 4.9, and reaches a value of 2270 Pa or 161 dB, which is higher than that observed for the previous cases with large spacing. The vortex-shedding components are not visible in the waterfall plot because their amplitudes are very small compared to that of the acoustic resonance.

The development of the vortex-shedding frequency and the normalized acoustic pressure as the flow velocity is increased are shown in Fig. 8. At low flow velocities, two vortex-shedding components are detected, which is to be expected from geometries with intermediate spacing ratio. However, as the flow velocity is increased, only the lower frequency component of vortex shedding persists and the higher frequency component disappears. These latter features exemplify those exhibited by cylinders with small spacing ratio, for which vortex shedding occurs at the low-frequency component only as illustrated in Fig. 1(b). Thus, it seems that as the Reynolds number is increased, the vortex-shedding process switches from the intermediate spacing regime, with two vortex-shedding components, to the small spacing regime, with one vortex-shedding component. In fact, these observations agree with the findings of other researchers

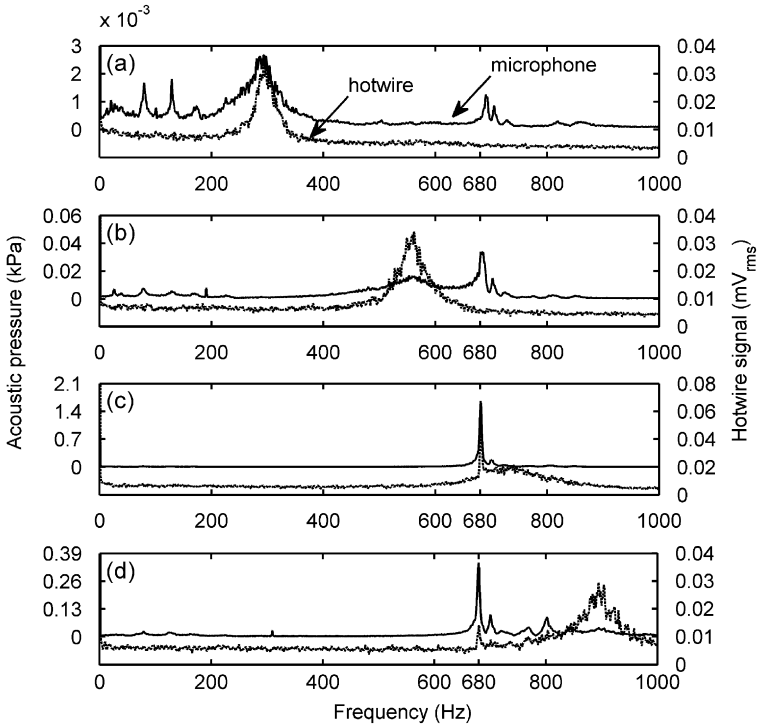

Fig. 5. Microphone and hot-wire spectra for $T/D = 2.5$: (a) $U_R = 1.92$; (b) $U_R = 3.68$; (c) $U_R = 5.03$ and (d) $U_R = 5.81$. The scale of acoustic pressure is given at the left hand side, and the scale of the hot-wire signal is on the right hand side.

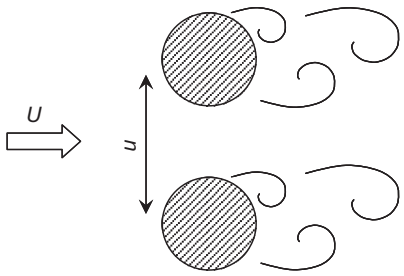

Fig. 6. Schematic of vortex-shedding pattern during acoustic resonance of two side-by-side cylinders with large spacing ratio.

who observed strong effect of the Reynolds number on the vortex-shedding regimes, especially when the spacing ratio is close to the boundaries between different regimes (Xu et al., 2003). As can be seen from Fig. 1(b), the present geometry is very close to the boundary between the small and the intermediate spacing ranges, which explains the observed change in the vortex-shedding features as the Reynolds number is increased.

Returning to Fig. 8, the two Strouhal numbers observed in this case are 0.12 and 0.36. Although these values are within the data range reported in the literature, they are slightly above the mean values shown in Fig. 1(b). This difference from the mean value is likely caused by the relatively high blockage ratio, which increases the velocity at flow separation. If a flow velocity based on the unobstructed flow area at the cylinders is used, these Strouhal numbers become 0.1 and 0.3, which are precisely the average values shown in Fig. 1(b). In order to eliminate any confusion related to the method used to correct the blockage effect, *all results in this paper are based on the upstream flow velocity.*

As can be seen in Fig. 8, the onset of resonance and the lock-in range do not correspond to either of the Strouhal numbers observed before the onset of resonance. Instead, the resonance occurs at an intermediate value between these

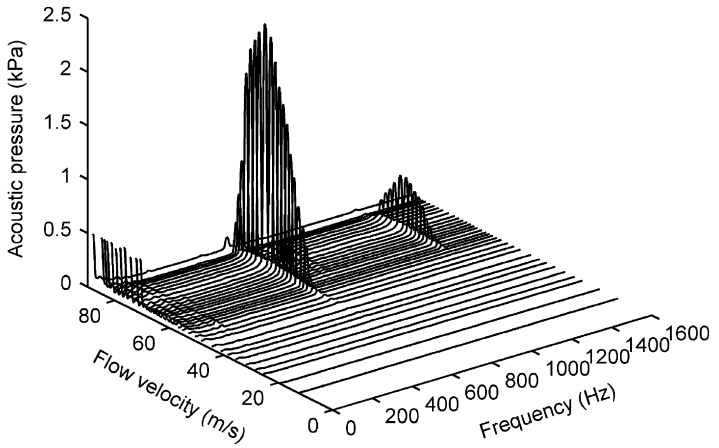

Fig. 7. Pressure spectra for the two side-by-side cylinders for $T/D = 1.25$ over the whole range of flow velocity.

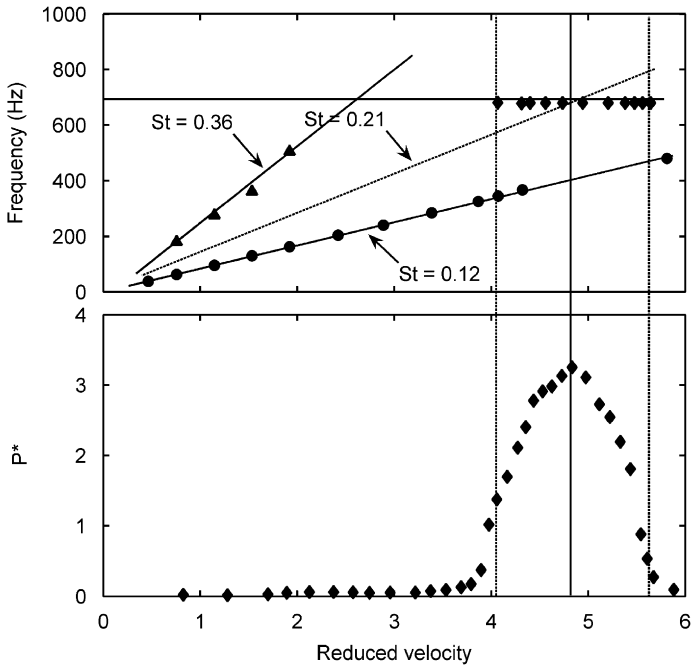

Fig. 8. Aeroacoustic response of the two side-by-side cylinders with $T/D = 1.25$ and $D = 21.8$ mm: ●, ▲, vortex-shedding frequencies measured by the hot-wire; ◆, first acoustic resonance mode frequency and magnitude.

two original Strouhal numbers. Also note that despite the smallness of the gap between the cylinders, the lock-in resonance is very intense; it is wider and produces higher normalized acoustic pressure than those observed for the case with large spacing.

Interestingly, after the lock-in resonance subsides near $U_R = 5.6$, the low-frequency component of vortex shedding is recovered and its frequency is clearly still lower than the acoustic resonance frequency. Parker and Stoneman (1989) describe this behaviour as "locking-up" for resonances that occur above a natural vortex-shedding frequency. Based on the present results, it appears that the resonant sound field synchronizes the vortex-shedding process from both cylinders and thereby eliminates the biased flow phenomenon and its associated dual vortex-shedding feature. Under these conditions, the sound-synchronized vortex shedding, as illustrated in Fig. 6, is likely to occur at an intermediate Strouhal number between the two Strouhal numbers associated with the biased flow. It is logical to expect this

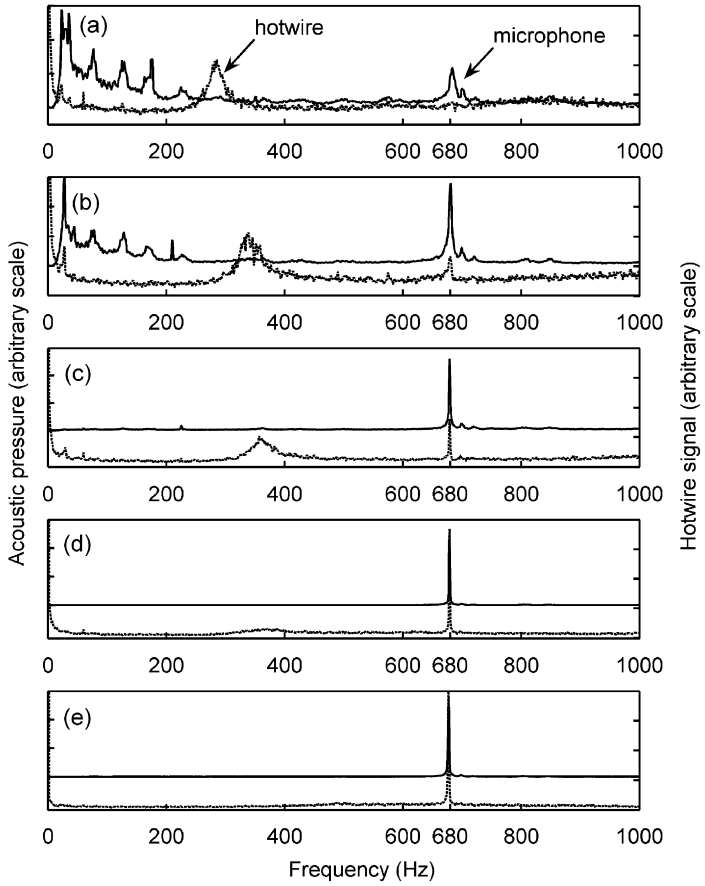

Fig. 9. Microphone and hot-wire spectra for $T/D = 1.25$: (a) $U_R = 3.39$; (b) $U_R = 4.07$; (c) $U_R = 4.32$; (d) $U_R = 4.56$ and (e) $U_R = 4.94$.

intermediate Strouhal number to be close to the *single Strouhal number observed at large spacing ratios*, and therefore, it can be represented in Fig. 1(b) by extrapolating the horizontal Strouhal number line for large spacing ratios to the range of small spacing ratios. In fact, Fig. 8 shows that the Strouhal number corresponding to the maximum normalized pressure is about 0.21, which is very close to that observed for large spacing ratios as illustrated in Figs. 1(b) and 4.

Typical hot-wire and microphone spectra are shown in Fig. 9 for several flow velocities corresponding to before and during the occurrence of acoustic resonance. Before the onset of resonance, Fig. 9(a), the lower vortex-shedding frequency is clearly visible near $f = 280$ Hz, but the higher one is not present. The spectra shown in Figs. 9(b)–(d) clearly illustrate the flow development into the lock-in region as the reduced velocity is increased from 4.1 to 4.6. The hot-wire spectra in Figs. 9(b) and (c) indicate the presence of both the lower vortex-shedding frequency and the narrow banded peak corresponding to the first acoustic mode. As the narrow banded resonance peak becomes stronger, the wide banded vortex-shedding component becomes weaker and totally subsides while it is still far removed from the resonance frequency. In other words, the vortex-shedding peak in the hot-wire spectra neither merges into the acoustic resonance peak nor becomes sharper when the resonance is initiated. These features suggest that the acoustic resonance mechanism is not related to the vortex-shedding component observed before the onset of resonance. Further increases in the flow velocity, and thereby in the acoustic pressure as well, completely suppress the lower vortex-shedding component in the hot-wire signal and produce a narrow-banded component at the resonance frequency; indicating complete transition from the biased flow in Fig. 1(a) to the synchronized flow illustrated in Fig. 6. During the initial phase of the lock-in range, corresponding to Figs. 9(b) and (c), both synchronized vortex shedding and biased flow are expected to co-exist, however, in the absence of flow visualization due to the high flow velocity and oscillation frequency, it is not clear whether this coexistence is concurrently or alternatively.

6. Results of the intermediate spacing cases

For intermediate spacing ratios, it has been shown in the literature that the bistable biased flow is composed of a narrow wake shed from one cylinder and a wide wake shed from the other cylinder. This flow pattern exhibits a flip-flop behaviour as described by Kim and Durbin (1988). In the present experiment, this was verified by placing a hot-wire within the biased jet between the two cylinders. At some time instant, the hot-wire would be located inside the wide wake and therefore be exposed to a low flow velocity. However, after the flow flips to the other side, the hot-wire probe would be positioned in the jet issuing between the two cylinders and thereby exposed to the high jet velocity. The hot-wire signal would therefore be expected to exhibit step like variations with time. Fig. 10 shows a typical time signal from a hot-wire located at $X/D = 1.5$ and $Y/D = 0.55$ for $T/D = 1.46$ and a reduced velocity of 2.14. This signal clearly shows that the flow at this spacing ratio exhibits strong bistable flow features before the onset of acoustic resonance.

The aeroacoustic response of the case with $T/D = 1.46$ is shown in Fig. 11. Since the case of $T/D = 1.35$ gave similar results to that of $T/D = 1.46$, it is not discussed here as the present case is representative of both. The high- and low-frequency components of vortex shedding exist throughout the flow velocities tested until the onset of resonance. These vortex-shedding frequencies have Strouhal numbers of 0.14 and 0.38, and can be seen in the hot-wire spectrum shown in Fig. 12(a) near $f = 250$ and 600 Hz, respectively. The spectra shown in Fig. 12(b) correspond to a reduced flow velocity

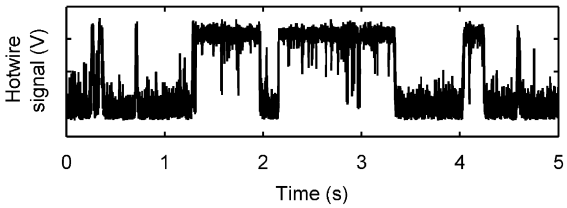

Fig. 10. Typical time signal from the hot-wire probe at $X/D = 1.5$ and $Y/D = 0.55$ for the case of $T/D = 1.46$ at $U_R = 2.14$. The high velocity shows that the probe is within the jet produced between the two cylinders, and the low velocity corresponds to when the probe is inside the wide wake.

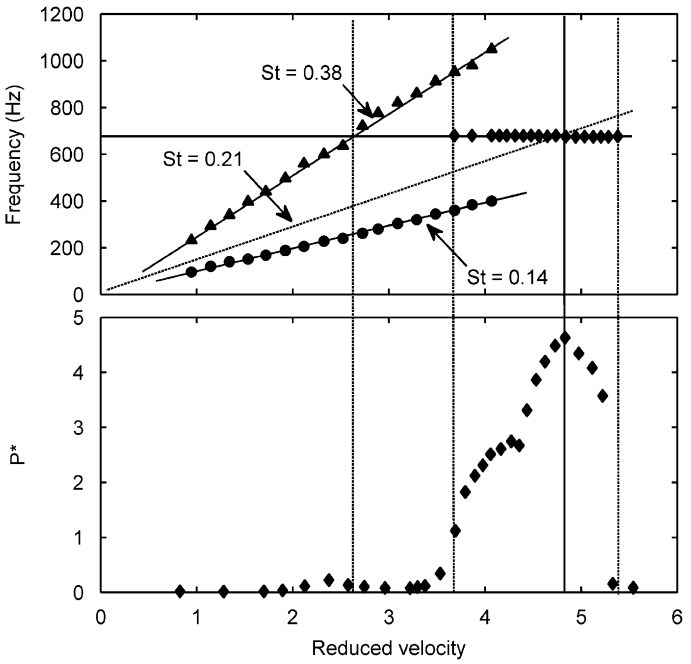

Fig. 11. Aeroacoustic response of the two side-by-side cylinders with $T/D = 1.46$ and $D = 21.8$ mm: ●, ▲, vortex-shedding frequencies measured by the hot-wire; ◆, first acoustic resonance mode frequency and magnitude.

of 4.06, which is within the initial phase of the lock-in range. Although the hot-wire signal shows a spectral peak at the acoustic resonance frequency, the bistable vortex-shedding components are still discernible. Referring again to Fig. 11, a strong acoustic resonance with a wide range of lock-in occurs at an intermediate Strouhal number. The spectra in Fig. 12(c) are taken at $U_R = 4.94$, which is close to the maximum SPL. They show high amplitude excitation of the first acoustic mode, and only one visible narrow frequency peak in the hot-wire data corresponding to the frequency of the first acoustic mode. Thus, Fig. 12(c) indicates that the flow is fully locked-in, or coupled with the resonant sound field.

As shown in Fig. 11, the resonance range for the spacing ratio $T/D = 1.46$ appears to consist of two resonance regimes separated by a kink in the amplitude curve. The resonance during the first regime, $3.5 < U_R < 4.4$, has been found to be intermittent. This intermittency is clearly depicted in Fig. 13; showing a typical time signal of the microphone at $U_R = 4.1$, which corresponds to Fig. 12(b). Note the amplitude modulation of the signal, which indicates that the acoustic resonance, or the flow–acoustic coupling, has not been fully established. When the reduced velocity is

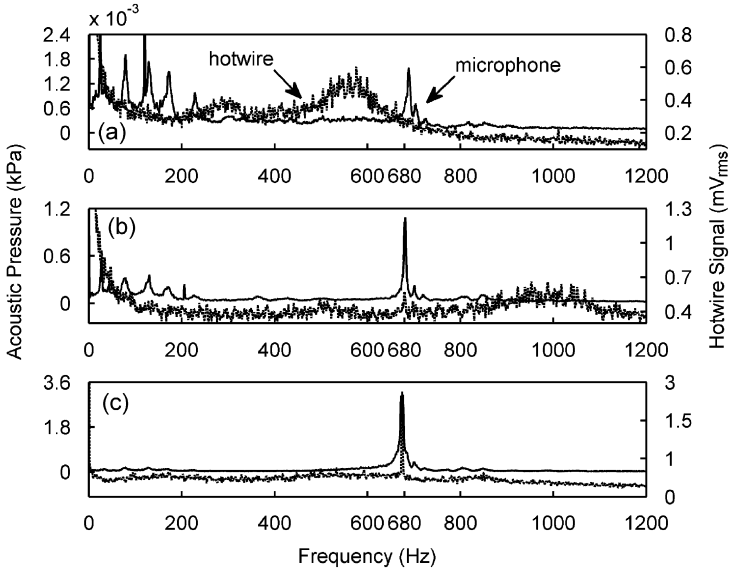

Fig. 12. Microphone and hot-wire spectrum for $T/D = 1.46$: (a) $U_R = 2.32$; (b) $U_R = 4.06$ and (c) $U_R = 4.94$.

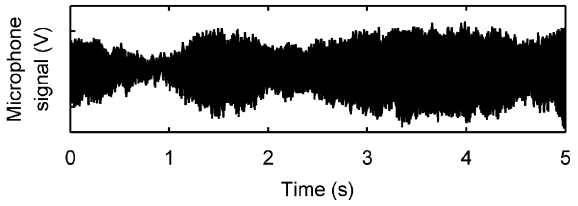

Fig. 13. Microphone time signal for $T/D = 1.46$ at $U_R = 4.11$.

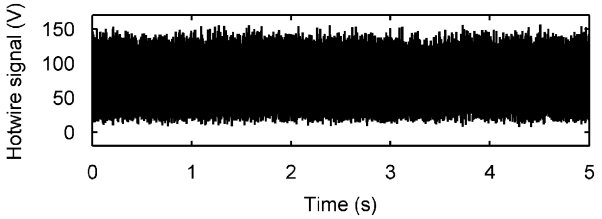

Fig. 14. Typical time signal from the hot-wire probe at $X/D = 1.5$ and $Y/D = 0.55$ for the case of $T/D = 1.46$ at $U_R = 4.94$ during acoustic resonance.

increased beyond the kink observed near $U_R = 4.4$, the acoustic resonance becomes stronger and much more persistent, as can be seen from Fig. 14, which shows the signal from a hot-wire positioned at a location similar to that corresponding to Fig. 10. This signal does not exhibit step-like variations as those observed in Fig. 10 for the bistable biased flow. Thus, the kink in the dimensionless acoustic pressure shown in Fig. 11 seems to mark the transition from intermittent resonance to fully developed acoustic resonance with persistent flow–acoustic coupling. The dimensionless sound pressure generated during this fully developed resonance reaches a large value of about 4.7, which corresponds to 164 dB. As in the small spacing case, the Strouhal number corresponding to this maximum acoustic pressure is 0.21, which is an intermediate value between the low- and the high-frequency components associated with bistable flow.

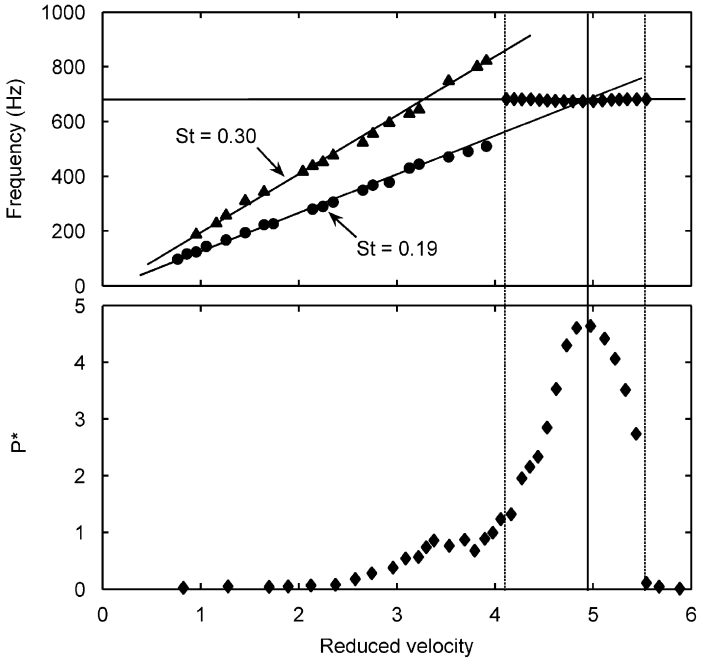

Fig. 15. Aeroacoustic response of the two side-by-side cylinders with $T/D = 1.75$ and $D = 21.8$ mm: ●, ▲, vortex-shedding frequencies measured by the hot-wire; ◆, first acoustic resonance mode frequency and magnitude.

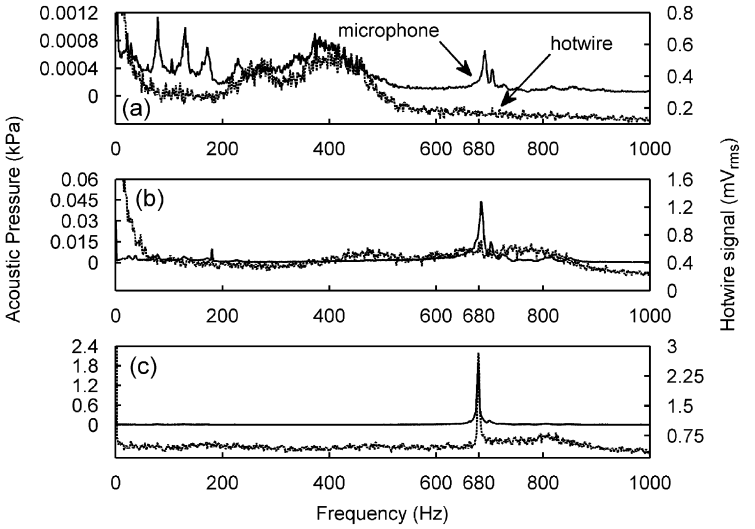

Fig. 16. Microphone and hot-wire spectra for $T/D = 1.75$: (a) $U_R = 2.04$; (b) $U_R = 3.50$ and (c) $U_R = 5.02$.

Thus, the occurrence of acoustic resonance synchronizes the wakes of both cylinders, and therefore the vortex shedding in both wakes become synchronized and of comparable strength. Comparison of Figs. 10 and 14, for example, clearly indicates that this synchronization eliminates the bistable biased flow and the dual-frequency phenomena, which is associated with the wide and narrow wakes observed before the onset of resonance. The acoustic resonance therefore occurs at an intermediate Strouhal number, which approximates that observed for large spacing side-by-side cylinders. This intermediate Strouhal number is indicated in Fig. 1(b) by the horizontal line extrapolated from the large spacing regime.

As in the previous case, $T/D = 1.25$, the flow pattern in the initial phase of lock-in is expected to exhibit both features of synchronized vortex shedding and bistable flow due to the intermittent nature of acoustic resonance as illustrated by the microphone signal in Fig. 13.

The aeroacoustic response for the case of $T/D = 1.75$ is shown in Fig. 15. In this case, the higher and the lower vortex-shedding frequencies exist throughout the non-resonant velocity range, up to $U_R = 4$. The high-frequency vortex-shedding component occurs at a Strouhal number of 0.3 and seems to pass by the acoustic mode frequency without causing a lock-in. However, near the velocity of frequency coincidence, $U_R = 2.8$–3.5, Fig. 15 shows some enhancement in the dimensionless pressure of the first mode. This enhancement seems to be caused by the higher vortex-shedding component.

Fig. 16 shows typical hot-wire and microphone spectra taken at several flow velocities. The two vortex-shedding components can be seen in the hot-wire spectra in Fig. 16(a) near 260 and 400 Hz, and in Fig. 16(b) near 470 and 750 Hz. The enhancement of the first acoustic mode caused by the broad banded, high-frequency vortex-shedding component can be seen in the microphone signal shown in Fig. 16(b). As the velocity is further increased, the lock-in with the first acoustic mode begins at a reduced velocity near 4, as shown in Fig. 15. The maximum dimensionless sound pressure observed in this case is about 4.7 or 165 dB, which is higher than those observed in all previous cases. Because the spacing ratio of this case is closer to the boundary of large spacing regime, the occurrence of acoustic resonance is not as clearly identified to occur at an intermediate Strouhal number, as in the previous cases with $T/D = 1.25$ or 1.46. However, the spectra shown in Fig. 16(c) indicate that the wake flow is fully coupled with the resonant sound field.

7. Concluding remarks

Flow-excited acoustic resonance of two side-by-side circular cylinders has been investigated experimentally. The test set-up has been shown to exhibit the main features observed in the literature for various spacing ratios between the cylinders, including the bistable biased flow phenomenon.

Vortex shedding from two side-by-side cylinders with *large spacing ratios*, $T/D = 2.5$ and 3.0, occurs at a single Strouhal number of 0.21, agreeing well with the values reported in the literature. Acoustic resonance of the wind tunnel first acoustic mode is excited by the vortex shedding observed before the onset of resonance. Therefore, the Strouhal number observed before the onset of resonance, $St = 0.21$, should be used for the purpose of designing against acoustic resonance when the spacing ratio is classified as large.

For small and intermediate spacing ratios, $T/D < 2.2$, the wakes are found to exhibit bistable flow features as those reported in the literature. Two Strouhal numbers of vortex shedding are observed before the onset of resonance. Acoustic resonance is not excited at either of those Strouhal numbers. Instead, it is excited at an intermediate Strouhal number which lies between those corresponding to the bistable flow regimes. It is concluded that the resonant sound field synchronizes the flow in the wakes of the cylinders and thereby eliminates the bistable biased flow. For this reason, acoustic resonances occur at an intermediate Strouhal number, which approximates that corresponding to vortex shedding from side-by-side cylinders with large spacing.

For the purpose of designing against acoustic resonance for small and intermediate spacing ratios, it is clear from the present results that using the higher Strouhal number of the bistable flow would result in overly conservative design. On the other hand, the use of the lower Strouhal number would result in designs, which are *not* conservative. Design engineers should therefore use an average Strouhal number value of 0.2, as indicated in Fig. 1(b), to predict and avoid acoustic resonances. As mentioned earlier, because of the relatively large blockage ratio, the Strouhal numbers measured in the present experiments are slightly higher than those reported in the literature. For this reason, the Strouhal numbers observed in the present experiments are considered to be somewhat conservative.

References

Alam, M., Moriya, M., Sakamoto, H., 2003. Aerodynamic characteristics of two side-by-side circular cylinders and application of wavelet analysis on the switching phenomenon. Journal of Fluids and Structures 18, 325–364.

Bearman, P.W., Wadcock, A.J., 1973. The interaction between a pair of circular cylinders normal to a stream. Journal of Fluid Mechanics 61, 499–511.

Blevins, R.D., 1985. The effect of sound on vortex shedding from cylinders. Journal of Fluid Mechanics 161, 217–237.
Blevins, R.D., Bressler, M.M., 1993. Experiments on acoustic resonance in heat exchanger tube bundles. Journal of Sound and Vibration 164, 503–533.
Bruggeman, J.C., Hirschberg, A., Van Dongen, M.E.H., Wijnands, A.P.J., Gorter, J., 1991. Self-sustained aeroacoustic pulsations in gas transport systems: experimental study of the influence of closed side branches. Journal of Sound and Vibration 150, 371–393.
Fitzpatrick, J.A., 1986. A design guide proposal for avoidance of acoustic resonances in in-line heat exchangers. Journal of Vibrations, Acoustics, Stress and Reliability in Design—Transactions of the ASME 108, 296–300.
Hall, J.W., Ziada, S., Weaver, D.S., 2003. Vortex shedding from single and tandem cylinders in the presence of applied sound. Journal of Fluids and Structures 18, 741–758.
Hourigan, K., Welsh, M.C., Thompson, M.C., Stokes, A.N., 1990. Aerodynamic sources of acoustic resonance in a duct with baffles. Journal of Fluids and Structures 4, 345–370.
Kim, H.J., Durbin, P.A., 1988. Investigation of the flow between a pair of circular cylinders in the flopping regime. Journal of Fluid Mechanics 196, 431–448.
Lighthill, M.J., 1952. On sound generated aerodynamically: I. General theory. Proceedings of the Royal Society A 211, 564–587.
Mohany, A., Ziada, S., 2007. Effect of flow–sound interaction on the dynamic lift force of a single cylinder in cross-flow. Dynamics of Continuous, Discrete and Impulsive Systems, Series B 14 (58), 1–18.
Mohany, A., Ziada, S., 2006. A parametric study of the resonance mechanism of two tandem cylinders in cross-flow. ASME Pressure Vessel and Piping Conference, Vancouver, Paper No. ICPVT11-93085 (also Journal of Pressure Vessel Technology, in press).
Mohany, A., Ziada, S., 2005. Flow excited acoustic resonance of two-tandem cylinders in cross-flow. Journal of Fluids and Structures 21, 103–119.
Norberg, C., 2003. Fluctuating lift on a circular cylinder: review and new measurements. Journal of Fluids and Structures 17, 57–96.
NRC Information Notice 2002-26 Supplement 1, 2003. Additional Failure of Steam Dryer Cover Plate after a Recent Power Uprate. US Nuclear Regulatory Commission, Washington, DC July 2003.
Oengoeren, A., Ziada, S., 1998. An in-depth study of vortex shedding, acoustic resonance and turbulent forces in normal triangle tube arrays. Journal of Fluids and Structures 12, 717–758.
Oengoeren, A., Ziada, S., 1992. Vorticity shedding and acoustic resonance in an in-line tube bundle—Part II: acoustic resonance. Journal of Fluids and Structures 6, 293–309.
Parker, R., Pryce, D.C., 1974. Wake excited resonances in an annular cascade: an experimental investigation. Journal of Sound and Vibration 37, 247–261.
Parker, R., Stoneman, S.A.T., 1989. The excitation and consequences of acoustic resonances in enclosed fluid flow around solid bodies. Proceedings of the Institution of Mechanical Engineers 203, 9–19.
Price, S.J., Paidoussis, M.P., 1984. The aerodynamic forces acting on groups of two and three circular cylinders when subject to a cross-flow. Journal of Wind Engineering and Industrial Aerodynamics 17, 329–347.
Stoneman, S.A.T., Hourigan, K., Stokes, A.N., Welsh, M.C., 1988. Resonant sound caused by flow past two plates in tandem in a duct. Journal of Fluid Mechanics 192, 455–484.
Sumner, D., Wong, S.S.T., Price, S.J., Paidoussis, M.P., 1999. Fluid behavior of side-by-side circular cylinders in steady cross-flow. Journal of Fluids and Structures 13, 309–339.
Xu, S.J., Zhou, Y., So, R.M.C., 2003. Reynolds number effects on the flow structure behind two side-by-side cylinders. Physics of Fluids 15, 1214–1219.
Ziada, S., 2006. Vorticity shedding and acoustic resonance in tube bundles. Journal of the Brazilian Society of Mechanical Science and Engineering 28, 186–199.
Ziada, S., Buehlmann, E.T., Bolleter, U., 1989. Flow impingement as an excitation source in control valves. Journal of Fluids and Structures 3, 529–549.
Ziada, S., Oengoeren, A., Vogel, A., 2002. Acoustic resonance in the inlet scroll of a turbo-compressor. Journal of Fluids and structures 16, 361–373.
Ziada, S., Scott, A., Arthurs, D., 2006. Acoustic excitation by flow in T-junctions. Journal of Pressure Vessel Technology—Transactions of the ASME 129, 14–20.